

# Hierarchically branched diffusion models for efficient and interpretable multi-class conditional generation

Alex M. Tseng<sup>1</sup> Tommaso Biancalani<sup>1</sup> Max Shen<sup>1</sup> Gabriele Scalia<sup>1</sup>

## Abstract

Diffusion models have achieved justifiable popularity by attaining state-of-the-art performance in generating realistic objects, including when conditioning generation on labels. Current diffusion models are universally linear in nature, modeling diffusion identically for objects of all classes. For the multi-class conditional generation problem, we propose a novel, structurally unique framework of diffusion models which are hierarchically branched according to the inherent relationships between classes. In this work, we showcase several advantages of branched diffusion models. We demonstrate that branched models generate samples more efficiently, and are more easily extended to novel classes in a continual-learning setting. We also show that branched models enjoy a unique interpretability that offers insight into the modeled data distribution. Branched diffusion models represent an alternative paradigm to their traditional linear counterparts, and can have large impacts in how we use diffusion models for efficient generation, online learning, and scientific discovery.

## 1. Introduction

Diffusion models have gained major popularity as a method for generating data from complex data distributions (Sohl-Dickstein et al., 2015; Ho et al., 2020; Song et al., 2021). In recent years, diffusion models have shown notable success in generating images and videos (Dhariwal & Nichol, 2021; Ho et al., 2022), graphs (Niu et al., 2020; Jo et al., 2022), and tabular data (Kotelnikov et al., 2022). Due to the impressive quality of their generated samples, they have rapidly become a staple in the field of generative models.

The goal of a diffusion model—as with any generative

model—is to sample data according to some intractable distribution  $q_0(x)$ . Diffusion models define a forward-diffusion process through time  $t \in [0, T)$ , which slowly transforms the distribution  $q_0(x)$  into some noisy forward-diffused distribution  $q_t(x|x_0)$ . As  $t$  approaches the time horizon  $T$ , the noisy distribution approaches a *prior distribution*  $q_T(x|x_0) = \pi(x)$ , where  $\pi$  is a tractable distribution (independent of any specific starting  $x_0$ ) that can be sampled from easily. The *reverse-diffusion* process is then learned from the training data, and is typically parameterized by a neural network  $p_\theta(x_t, t)$  trained to effectively recover the posterior distribution  $p(x_{t-1}|x_t)$ . After training, the diffusion model can be used to sample objects from the original data distribution  $q_0$  (or ideally close to  $q_0$ ) by first sampling from  $\pi$ , and then following  $p_\theta$  from time  $T$  to time 0. Note that the time interval  $[0, T)$  on which diffusion is defined may be treated as a series of discrete time steps of unit length or as a continuous interval. In the discrete case, the diffusion model behaves in a Markovian fashion (Ho et al., 2020). In the continuous case, the diffusion process may be modeled by an underpinning stochastic differential equation (Song et al., 2021). Both the discrete and continuous frameworks have shown success, and both continue to be used today for different data modalities and generative problems (Austin et al., 2021; Hooeboom et al., 2021; Jo et al., 2022; Karras et al., 2022).

Although diffusion models are traditionally trained to sample unconditionally from  $q_0(x)$ , it is arguably much more useful in practice to perform *conditional generation*, where we wish to sample not from  $q_0(x)$ , but from  $q_0(x|y)$  (i.e. a sample conditioned on some label  $y$ ). It is *conditional* generation that has received the most popular attention in recent works. This includes image generation by class (Song et al., 2021; Dhariwal & Nichol, 2021), image/video synthesis from text (Rombach et al., 2021; Ho et al., 2022), and property-specific molecule generation (Lee et al., 2022).

Although diffusion models have attained impressive performance in many areas, they have also experienced some pitfalls. One major drawback of diffusion models is the high computational cost of sampling, due to the fact that samples must be generated iteratively from  $t = T$  to  $t = 0$ . To generate 50k ImageNet samples on an A100 GPU, for example,

<sup>1</sup>Department of Artificial Intelligence and Machine Learning, Research and Early Development, Genentech. Correspondence to: Alex M. Tseng <tseng.alex@gene.com>.

can take about 5 days (Rombach et al., 2021; Dhariwal & Nichol, 2021). Furthermore, even before diffusion models can be sampled from, they need to be trained on many time steps—and potentially many conditional classes (Ho et al., 2022)—to obtain sufficient coverage. This can be a crucial limitation in a continual-learning setting, where the emergence of new classes (which were not available during training) typically requires the whole model to be retrained (van de Ven & Tolia, 2019). Given the carbon emissions and energy consumption required by these neural networks, there is a dire need for more computationally efficient methods which avoid retraining large models where possible (Strubell et al., 2020; Patterson et al., 2021).

Furthermore, although diffusion models are now a popular generative technique, there is limited work (if any) that attempts to improve or take advantage of diffusion-model interpretability. Since a trained diffusion model learns about the distribution  $q_0$ , it stands to reason that some information about the underlying distribution may be extracted, such as the subtle relationships between data points of different classes. Being able to leverage a trained diffusion model to better understand the underlying data—even from a generative perspective—could be useful for many real-world problems, such as drug discovery.

In this work, we tackle the problem of multi-class conditional generation in diffusion models (i.e. generation of samples that are conditioned on one of many discrete labels). To address the above limitations of traditional models, we propose a novel structure of diffusion models which are hierarchically branched, where the branching structure reflects the inherent relationships between different classes. This directly contrasts with the current paradigm of diffusion models, which are universally treated as a purely linear process. In particular, we will highlight the following contributions:

- Branched diffusion models are far more computationally efficient for multi-class sample generation
- They are easily extended to generate new, never-before-seen data classes in an efficient and principled manner
- Their branching structure offers interpretability into the diffusion and generation processes
- They are flexibly applied to a variety of data types, any forward-diffusion scheme or noise schedule, and can be orthogonally combined with many other methods that improve diffusion-model efficiency

## 2. Related Work

Within the traditional diffusion-model setting, conditional generation by class label was first proposed in Song et al.

(2021), which applied conditional generation to continuous-time diffusion models. During sampling, input gradients from a pretrained classifier are added to the model output. This secondary term effectively *biases* the sampling procedure to generate a sample which is conditioned on some label  $y$ . An advantage of this method is modularity: a diffusion model needs to be trained only once, and different classifiers can be swapped in at will. Unfortunately, however, this method suffers from two main drawbacks: 1) because of the reliance on gradients, this method does not easily extend to discrete-time diffusion models; and 2) the external classifier needs to be trained on  $x_t$  at every stage of diffusion, even though  $x_t$  generally is not informative for any label  $y$  at larger  $t$  (i.e. later diffusion times).

Later on, Ho et al. (2021) proposed an alternative way to perform conditional generation by class label, which was termed “classifier-free conditional generation”. In this method, the reverse-diffusion neural network is given the class label  $y$  as an auxiliary input:  $p_\theta(x_t, t, y)$ . This method effectively combines the external pre-trained classifier from Song et al. (2021) and the diffusion model into one neural network, where the class label *guides* the generation of objects to specific classes. This method of conditional generation has achieved state-of-the-art performance in sample quality (Rombach et al., 2021; Ho et al., 2022). In contrast with the previous method, this strategy can be applied to both continuous- and discrete-time diffusion models. As a tradeoff, however, it loses modularity (i.e. we can no longer swap in different classifiers). It also is of dubious utility to supply labels at later diffusion times, as heavily diffused objects of distinct classes are generally indistinguishable from each other.

Tackling the problem of efficient sampling, several diverse methods have been proposed. Many have attempted to directly reduce the number of time steps that the iterative sampling process must go through. For example, specifically on discrete-time diffusion models, Song et al. (2021) encoded skip connections in the generation process, and Kong et al. (2020); Kong & Ping (2021); Watson et al. (2021) only performed generation at certain cleverly selected noise levels. Xiao et al. (2021) reparameterized the reverse-diffusion process to allow for more complex distributions in fewer generation steps. Separately, Dockhorn et al. (2021) improved on the sampling algorithm itself, thereby requiring fewer time steps for generation.

Other methods for efficient sampling have attempted to reduce not the number of time steps for generation, but the complexity of each step. Vahdat et al. (2021) and Rombach et al. (2021) trained diffusion models on a learned latent space of lower dimension than the input  $x$ . This reduces training time as well as sampling time simply by virtue of having the diffusion model operate on smaller-dimensional

inputs.

Importantly, all these previously proposed methods for improving training or sampling efficiency are orthogonal to the approach proposed in this work. Our method can be combined with any of these others for even higher efficiency.

### 3. Hierarchically branched diffusion models

In order to train a diffusion model to support multi-class conditional generation, we propose a hierarchically branched diffusion structure (Figure 1). For some data distribution  $q_0(x)$  which consists of many discrete classes, there are often inherent relationships between the classes. For example, if we consider the MNIST dataset of hand-written digits, images of 4s and 9s are more similar to each other on average than 4s and 0s. At later times in the diffusion process, images of 4s and 9s are sufficiently noisy that they are practically indistinguishable from each other. Symmetrically, it stands to reason that the reverse-diffusion process can be shared between 4s and 9s at these later times.

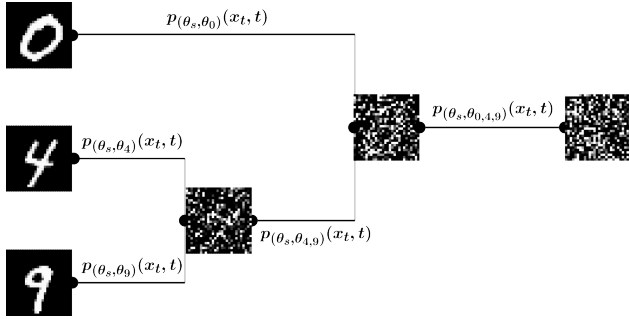


Figure 1. Schematic of a branched diffusion model. As opposed to a standard (linear) diffusion model, a multi-class branched diffusion model learns a hierarchical diffusion process to generate objects of distinct classes separately. Branches at the earliest diffusion times are unique to each class. Branches at later diffusion times are shared for classes which are similar to each other. In the figure above, diffusion occurs along the horizontal lines. The reverse-diffusion process is learned by a multi-task neural network (one output task for each branch) parameterized both by weights  $\theta_s$  that are shared across all branches, and weights  $\theta_i$  that are unique to each branch.

In general, suppose our dataset consists of a set of classes  $C$  (e.g. for MNIST,  $C = \{0, 1, \dots, 9\}$ ). Because some classes in  $C$  are more similar to other classes, we can construct a *hierarchy* of class similarities. A branched diffusion model mirrors this hierarchical structure, where the learned reverse-diffusion process is shared between closely related classes at later time intervals (i.e. large  $t$ , or early in the reverse-diffusion process). It is only at early times (i.e. small  $t$ ) that the reverse-diffusion process needs to be distinct for each class. The more closely related two classes are, the shorter

the unique branches are in the reverse diffusion at early  $t$ .

For  $|C|$  classes, there are  $2|C| - 1$  branches. Each branch  $b_i = (s_i, t_i, C_i)$  of the diffusion model is defined by a particular diffusion time interval  $[s_i, t_i)$  (where  $0 \leq s_i < t_i < T$ ) and a subset of classes  $C_i \subseteq C$  (where  $C_i \neq \emptyset$ ). Note that the branches are constrained such that:

1. Every class and time  $(c, t) \in C \times [0, T)$  can be assigned to exactly one branch  $b_i$  such that  $c \in C_i$  and  $t \in [s_i, t_i)$
2. There are  $|C|$  branches  $b_i$  where  $s_i = 0$  (this enforces that each class gets its own branch at the end of the reverse-diffusion process)
3. There is exactly one branch  $b_i$  where  $t_i = T$  (this enforces that all classes share the very beginning of the reverse-diffusion process)
4. The branches  $b_i$  form a rooted tree starting from  $t = T$  to  $t = 0$ .

The optimal branch definitions  $b_i$  for any dataset (regardless of modality) can be easily computed from the data alone, by forward diffusing each class and computing the time points at which classes become just noisy enough so that they are indistinguishable from each other (Supplementary Methods). They may also be entirely defined by prior domain knowledge if desired.

In practice, a branched diffusion model is implemented as one multi-task neural network, where each output task of the model predicts the reverse diffusion for a single branch  $b_i$ . The neural network includes parameters  $\theta_s$  which are shared across all branches/tasks, and parameters  $\theta_i$  which are unique to each branch  $b_i$ . The multi-task architecture allows the model to learn a distinct reverse-diffusion process for each branch, while the shared parameters allow the network to benefit from seeing the entire data distribution across all classes, without an explosion in model complexity.

Training a branched diffusion model follows nearly the same procedure as training a standard linear diffusion model (continuous or discrete time), except for each training example  $x^{(k)}$  of class  $c^{(k)}$ , we only perform gradient descent on the appropriate branch (i.e. model output task) (Algorithm 1).

To sample an object of a particular class  $c$ , we perform reverse diffusion starting from time  $T$  and follow the appropriate branch down (Algorithm 2).

We demonstrate our branched diffusion models on two datasets of different data modalities: MNIST handwritten digit images and a tabular dataset of several hand-engineered features for the 26 English letters of various fonts. We trained continuous-time branched diffusion models for both datasets. The branching structure was inferred from the

**Algorithm 1** Training a branched diffusion model

---

**Input:** training set  $\{(x^{(k)}, c^{(k)})\}$ , branches  $\{b_k\}$   
**repeat**  
  Sample  $(x_0, c)$  from training data  $\{(x^{(k)}, c^{(k)})\}$   
  Sample  $t \sim \text{Unif}(0, T)$   
  Forward diffuse  $x_t \sim q_t(x|x_0)$   
  Find branch  $b_i = (s_i, t_i, C_i)$  s.t.  $s_i < t \leq t_i, c \in C_i$   
  Gradient descent on  $p_{(\theta_s, \theta_i)}(x_t, t)[i]$  (on output task  $i$ )  
**until** convergence

---

**Algorithm 2** Sampling a branched diffusion model

---

**Input:** class  $c$ , trained  $p_\theta$ , branches  $\{b_k\}$   
  Sample  $\hat{x} \leftarrow x_T$  from  $\pi(x)$   
  **for**  $t = T$  to 0 **do**  
    Find branch  $b_i = (s_i, t_i, C_i)$  s.t.  $s_i < t \leq t_i, c \in C_i$   
     $\hat{x} \leftarrow p_\theta(\hat{x}, t)[i]$  (take output task  $i$ )  
  **end for**  
  Return  $\hat{x}$

---

data alone (Supplementary Tables S1–S5, Supplementary Methods). For our MNIST model, we visualized a random sample of digits generated from our branched diffusion model, and verified that we were able to generate distinct digits conditioned on their class (Supplementary Figure S1). For our tabular letter dataset, we followed Kotelnikov et al. (2022) and examined the distribution of generated features and their correlations. We found that the branched model generated letters that are realistic and true to the training data (Supplementary Figure S2). Notably, because of the branched structure, the conditional generation of a distinct class of data is extremely simple, and requires no more computation than an unconditional linear diffusion model.

To further confirm that our branched diffusion models generate high-quality samples, we also trained label-guided (linear) diffusion models on each dataset (Ho et al., 2021). Note that although Ho et al. (2021) called these “classifier-free” diffusion models, we will refer to them as “label-guided” in this work, since branched diffusion models also allow for conditional generation without the use of any external classifier. Our label-guided diffusion models were trained on the same data using a similar architecture and capacity (except single-task instead of multi-task). We computed the Fréchet inception distance (FID) for each class, comparing the branched diffusion models and their linear label-guided counterparts (Supplementary Figure S3). In general, the branched diffusion models achieved similar generative performance compared to the current state-of-the-art label-guided strategy. In many cases, the branched models even *outperformed* the label-guided models, likely due to the multi-tasking which can help limit inappropriate crosstalk between distinct classes. This establishes that branched diffusion models offer competitive performance

in terms of sample quality.

Although we will focus our later analyses on continuous-time diffusion models, we also trained a branched diffusion model in *discrete time* to generate distinct MNIST classes (Supplementary Figure S1). This illustrates the flexibility of branched diffusion models, as they are able to perform equally well in both continuous- and discrete-time diffusion settings.

## 4. Efficient sampling from branched diffusion models

Branched diffusion models offer significant improvements in computational efficiency when sampling from multiple classes. Sampling from a diffusion model is generally very computationally expensive due to the iterative nature of the model (i.e. sampling begins at time  $t = T$  and proceeds iteratively to  $t = 0$ ), as it cannot be parallelized for a single sample. In a branched diffusion model, however, much of the diffusion process is *shared* for many classes. Partially reverse-diffused intermediates at branch points can be cached and reused to generate samples for multiple classes. Note that although a branched diffusion model takes the same amount of computation to generate samples of a *single* class compared to a standard linear model, branched models enjoy significant savings in computational efficiency when sampling *multiple* classes.

Table 1. Efficiency of multi-class conditional generation

DATASET	LINEAR MODEL	BRANCHED MODEL
MNIST	$78.73 \pm 0.11$	<b><math>37.30 \pm 0.03</math></b>
LETTERS	$110.42 \pm 0.14$	<b><math>67.54 \pm 0.04</math></b>

Averages and standard errors are shown over 10 trials each. All values are reported as seconds.

In order to quantify the efficiency offered by branched diffusion models, we generated one batch of each class in our branched models, and compared the time taken to a linear diffusion model of identical architecture and capacity (Table 1). Our branched diffusion models enjoyed a significant speedup. Note that the speedup factor for multi-class sample generation depends on the branching structure between the classes: if there are many similar classes, they can share more of the reverse-diffusion process, yielding more computational savings.

## 5. Extending branched diffusion models to novel classes

In addition to efficient generation, the unique hierarchical structure of branched diffusion models allows new classes to be added easily. Suppose a branched diffusion model



has been trained on classes  $C$ , and now a never-before-seen class  $c'$  has been introduced. Instead of retraining the diffusion model from scratch on  $C \cup \{c'\}$ , a branched diffusion model can be easily extended by introducing a new branch while keeping the other branches the same (assuming  $c'$  is sufficiently similar to some existing class).

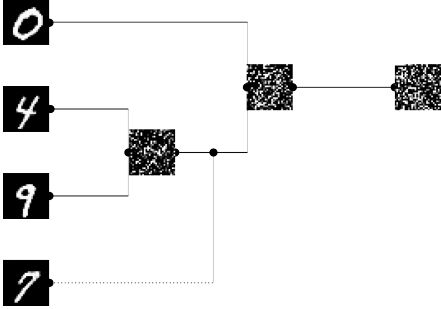


Figure 2. Extending a branched model to new classes. We demonstrate the ability of branched diffusion models to easily accommodate new classes after training on existing classes. We started with a branched model trained to generate three MNIST digits (0, 4, and 9). To generate a brand new digit class (7), the model was easily extended by adding on a single new branch. This new branch was trained only on 7s and over a short diffusion time interval.

To illustrate this extendability, we trained a small branched diffusion model on three MNIST classes: 0s, 4s, and 9s. We then introduced a new digit class: 7. In order to accommodate this new class, we added a single new branch to the diffusion model (Figure 2). We then fine-tuned *only the newly added branch*, freezing all shared parameters  $\theta_s$  and parameters for other output tasks. That is, we only trained on 7s, and only on times  $t \in [s_i, t_i]$  for the newly added branch. After fine-tuning, our branched diffusion model was capable of generating high-quality 7s *without affecting the ability to generate the other digits* (Figure 3, Supplementary Figure S4).

In contrast, if we take a label-guided (linear) diffusion model (also trained on 0s, 4s, and 9s), it is much more difficult to extend the model to accommodate a new digit class. After fine-tuning the label-guided model on 7s, the model suffered from *catastrophic forgetting* (van de Ven & Tolias, 2019): it largely lost the ability to generate the other digits, and generated almost all 7s for any label (Figure 4, Supplementary Figure S4). In order for the linear model to retain its ability to generate pre-existing digits, it must be trained on the *entire* dataset, which is far more inefficient, particularly when the number of classes is large. Whereas training the singular new branch on the branched diffusion model took less than 30 seconds, retraining a linear model on all data would require 3.5 minutes.

Notably, in our extension of the branched diffusion model,

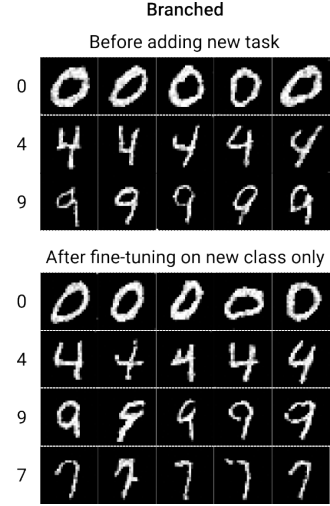


Figure 3. Fine-tuning branched diffusion models on new classes. After extending a pretrained branched diffusion model by adding a new branch for a new class, we can easily train that new branch to conditionally generate the new class without affecting the generation of any other pre-existing classes. On our MNIST example, after training on only 7s, the branched model was able to generate high-quality examples of the new class, while leaving its generation of other digits completely unaltered.

we were able to generate high-quality digit samples even with a very simplistic strategy. Specifically, we only added and trained a *single* branch. Although we were able to generate high-quality 7s already from this strategy, performance may be boosted even more by fine-tuning on *all* branches in which 7 (or in general, the new class  $c'$ ) is a part of (i.e. unfreeze and fine-tune all output tasks whose branches  $b_i$  have  $c' \in C_i$ ). For these upstream branches  $b_i$  (i.e. at later time points in diffusion) which reverse diffuse over more than only  $c'$  (i.e.  $C_i \setminus \{c'\} \neq \emptyset$ ), we found anecdotally that fine-tuning can be performed on only examples of  $c'$ , and the model still did not forget how to generate the other classes. This is likely due to the fact that in a branched model, the last branch in reverse diffusion is unique for each individual class, and reverse diffusion at upstream branches is nearly identical between distinct classes (by design). Note that even if fine-tuning is done on all classes for all  $b_i$  where  $c' \in C_i$ , the branched diffusion model is still more efficient to extend than a linear model because most branches will not require training on all classes in  $C$ .

This highlights the advantage of branched diffusion models to accommodate new classes efficiently (i.e. requiring little training) and cleanly (i.e. without affecting the generation of pre-existing classes).

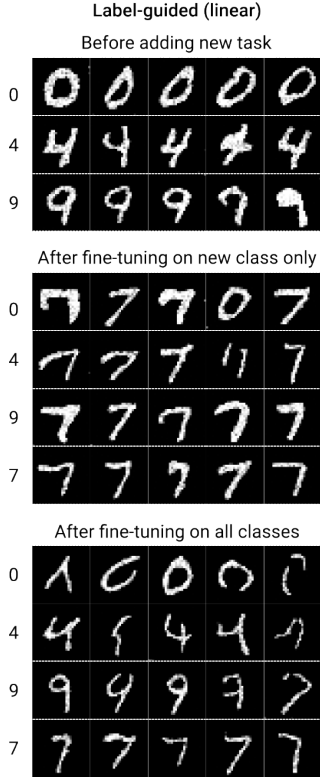


Figure 4. Fine-tuning linear diffusion models on new classes. Whereas branched diffusion models could accommodate a new class by efficiently training on only that class for a short time interval, fine-tuning on only 7s caused the label-guided model to almost entirely forget about other digits (even though the label of other digits were being fed to the model during sample generation). In order to retain the linear model’s ability to generate all classes, retraining must be performed on all classes over all diffusion time intervals. Even after retraining on all classes, the linear model’s generation of old tasks still experienced inappropriate influence from the new task.

## 6. Interpretability of branched diffusion models

In addition to efficiency and extendability, branched diffusion models also offer very unique interpretations into the underlying data distribution. By encoding the relationship between classes explicitly as branch points in the diffusion process, branched diffusion models can reveal insight into common features between classes, and can even generate analogous objects between different classes.

### 6.1. Hybrids at branch points

In a branched diffusion model, branch points act as “minimal times of indistinguishability”. In the forward-diffusion process, two branches meet at a branch point when the

classes become sufficiently noisy such that they cannot be distinguished from each other. Symmetrically, in the reverse-diffusion process, branch points are where distinct classes split off and begin reverse diffusing along different trajectories. Thus, for two similar classes (or two sets of classes), the reverse-diffusion intermediate at a branch point naturally encodes features which are shared (or otherwise intermediate or interpolated) between the two classes (or sets of classes).

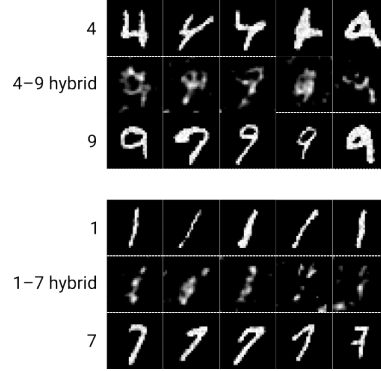


Figure 5. Interpretable MNIST hybrids at branch points. Generated objects at branch points between closely related classes show characteristics which are shared between the classes. From our branched diffusion model trained on MNIST images, we show some examples of hybrids between the digits classes 4 and 9 (top), and between the digit classes 1 and 7 (bottom). Each hybrid digit we show is the reverse-diffusion starting point for both images above and below it. We applied a small amount of Gaussian smoothing to the hybrids for ease of viewing.

Firstly, we can visualize hybrid intermediates as partially reverse-diffused objects right before a branch splits into two distinct digit classes. Formally, for two classes  $c_1$  and  $c_2$ , let  $t_b$  be the first branch point (earliest in diffusion time) in which  $c_1$  and  $c_2$  are both in the same branch. We define a *hybrid object* between classes  $c_1$  and  $c_2$  as the generated object from reverse diffusion following Algorithm 2 from time  $T$  until time  $t_b$  for either  $c_1$  or  $c_2$  (it does not matter which, since we stop at  $t_b$ ).

For example, on our MNIST branched diffusion model, hybrids tend to show shared characteristics that underpin both digit distributions (Figure 5). On our branched model trained on tabular data, we see that hybrids tend to interpolate between distinct feature distributions underpinning the two classes, acting as a smooth transition state between the two endpoints (Figure 6).

Note that although a branched diffusion model can successfully generate distinct classes even with very conservative branch points (i.e. late in diffusion time), the interpretability of the hybrid intermediates is best when the branch points

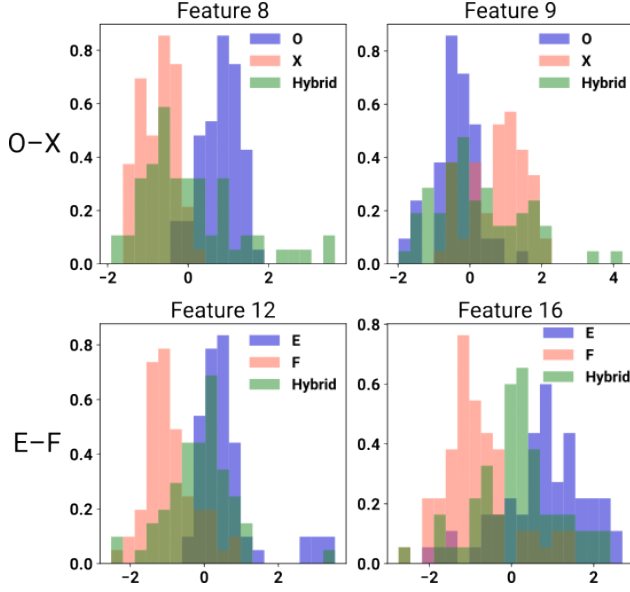


Figure 6. Interpretable letter hybrids at branch points. From our branched diffusion model trained on tabular letters, we show the distribution of some features between two pairs of classes: O and X (top), and E and F (bottom). In each plot, we also show the distribution of that feature in the generated hybrids from the branch point between the two classes. In each pair of letters, although the distributions of these features are rather distinct for each letter, the generated hybrid acts as an intermediate, which effectively interpolates between the two distributions.

are *minimal* (earliest in diffusion) times of indistinguishability. Taken to the extreme, branch points close to  $t = T$  encode no shared information between classes whatsoever, as the distribution of objects at time  $T$  is independent of class.

## 6.2. Transmutation between classes

In a diffusion model, we can traverse the diffusion process both forward and in reverse. Because branched diffusion models encode shared or interpolated characteristics between classes at branch points, this allows for a unique ability to perform *transmutation* (or *analogous* conditional generation) between classes. That is, we can use branched diffusion models to start with an object from one class, and generate the analogous, corresponding object in a different class. Formally, say we have an object  $x_1$  of class  $c_1$ . We wish to transmute this object into the analogous object of class  $c_2$ . Let  $t_b$  be the first branch point (earliest in diffusion time) in which  $c_1$  and  $c_2$  are both in the same branch. Then in order to perform transmutation, we first forward diffuse  $x_1$  to  $x_b \sim q_{t_b}(x|x_1)$ . Then, we reverse diffuse to generate an object of class  $c_2$  (Algorithm 2), as if we started at time  $t_b$  with object  $x_b$ .

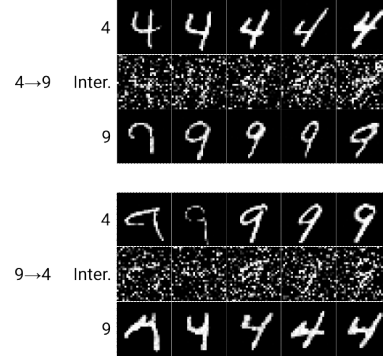


Figure 7. Transmutation between MNIST classes. Branched diffusion models offer a unique method for transmuting one class to another, by forward-diffusing from an object to a branch point, and reverse-diffusing down to a different class. This generates the analogous object in a different class. From our branched diffusion model trained on MNIST images, we show some examples of 4s transmuted to 9s (top), and 9s transmuted to 4s (bottom). We also show the diffusion intermediate  $x_b$  at the branch point. We see that in this transmutation process, digits which are slanted tend to transmute to digits in other classes which are also slanted.

On our MNIST branched diffusion model, we transmuted between 4s and 9s (Figure 7). Intriguingly, the model learned to transmute based on the *slantedness* of a digit. That is, slanted 4s tend to transmute to slanted 9s, and *vice versa*. To further quantify the analogous conditional generation between classes, we transmuted between letters on our tabular branched diffusion model (Figure 8). Transmuting between V and Y (and *vice versa*), we found that all features showed a positive correlation when comparing the value of the feature before and after transmutation. That is to say, letters with a larger feature value tended to transmute to letters also with a larger feature value, *even if the range of the feature is different between the two classes*. Over all features, we found that many were strongly correlated before and after transmutation. This underscores the ability of branched diffusion models to transmute objects of one class to the *analogous* object of a different class.

Together with our exploration of hybrid intermediate states, transmutation exemplifies the interpretability that is offered by branched diffusion models.

## 7. Discussion

In this section, we explore some of the tradeoffs and caveats of branched diffusion models.

Firstly, branched diffusion models represent a tradeoff between training and sampling complexity. Because branched models separate the diffusion process into many branches (many of which overlap in diffusion time), they typically

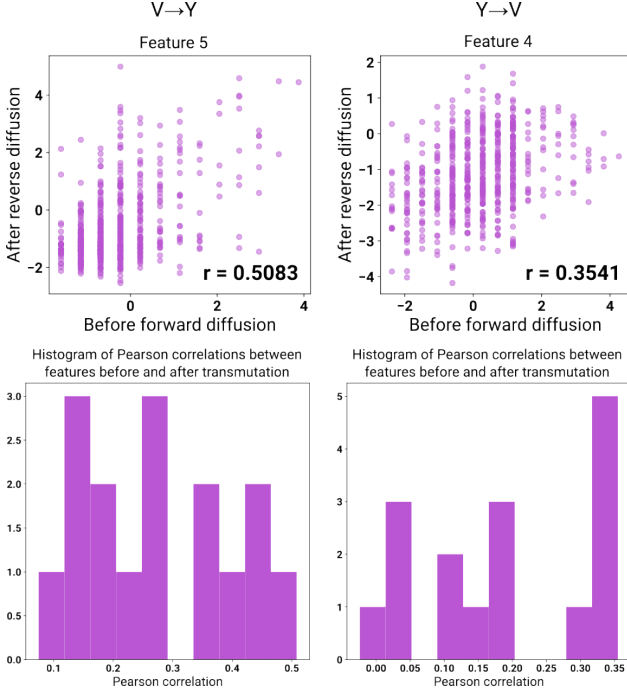


**Figure 8.** Transmutation between letter classes. From our branched diffusion model trained on tabular letters, we show the scatterplots of some feature values before and after transmutation from Vs to Ys (left), or Ys to Vs (right). We achieved a high Pearson correlation between the feature values before versus after transmutation, suggesting that the transmuted samples are analogous to their original counterparts. We also show a histogram of Pearson correlations over all 16 features in either transmutation direction; these correlations are strongly biased toward very positive values.

require more parameters and more training time than their linear counterparts. Notably, however, the multi-task architecture allows for significant savings in terms of model size, and although we found that training branched diffusion models took more epochs than a linear model, the training time was far lower than the expected time based solely on total branch length or model capacity (Supplementary Table S6). Most importantly, branched diffusion models enjoy significant savings in computational efficiency during *sampling*. For most generative models, one can usually expect that far more time will be spent sampling from them than training them, and so branched models can be extremely rewarding on average. Additionally, branched diffusion models can easily be combined with the many other methods for improving sampling efficiency proposed in other works (Section 2), which may allow for even more computational savings.

Another limitation of branched diffusion models is their requirement for branch points to be times of indistinguishability between classes. For most datasets, this poses no issue. This can, however, be challenging for certain image

datasets where the subject of the image (which defines the class) can be in very different parts of the image, particularly when the data may be sparse for certain classes. For example, a branched model trained to conditionally generate images of dogs and cats may have difficulties if there are few examples of dogs and cats in the same location in the images. For datasets like MNIST, the digits are all roughly in the center of the image, thus obviating this problem. Of course, images and image-like data are the only modalities that suffer from this problem, and branched diffusion can easily accommodate all other modalities such as tabular data (as shown), graphs, and text. Furthermore, this limitation on images may be avoided by diffusing in latent space.

## 8. Conclusion

In this work, we proposed a novel form of diffusion models which introduces branch points to explicitly encode the hierarchical relationship between distinct data classes. Branched diffusion models offer an alternative framework of conditional generation for discrete classes. They are also flexibly applied to many traditional diffusion-model paradigms (e.g. continuous or discrete time, different noise schedules and definitions of the noising process, etc.). Compared to the traditional linear diffusion models, we showcased several advantages offered by branched models.

Firstly, it is far more efficient to sample multiple classes from a branched diffusion model than from a linear one. Particularly given the tendency for large generative models to be sampled from much more often than they are trained, this computational efficiency is a great benefit that reduces the carbon footprint and power consumption of these otherwise computationally expensive neural networks. We also showed that branched models are easily extendable to new, never-before-seen classes through a short and efficient fine-tuning step which does not lead to catastrophic forgetting of pre-existing classes. This can enhance diffusion-model training in online-learning settings. Finally, we showed that branched diffusion models can offer some insights into interpretability. Namely, reverse-diffusion intermediates at branch points are hybrids which encode shared or interpolated characteristics of multiple data classes. Furthermore, this allows branched models to transmute objects from one class into the analogous object in another class. The interpretability of these models can thus be very useful for data exploration and scientific discovery. To our knowledge, this work is one of the few which explores the interpretability of diffusion models, and the only one which directly attempts to improve it.

Further exploration in the physical structure of diffusion models (e.g. branched vs linear) may continue to have resounding impacts in how these models are used in many areas.



## References

- Austin, J., Johnson, D. D., Ho, J., Tarlow, D., and Berg, R. V. D. Structured denoising diffusion models in discrete state-spaces. *Advances in Neural Information Processing Systems*, 22:17981–17993, 7 2021. ISSN 10495258. doi: 10.48550/arxiv.2107.03006. URL <https://arxiv.org/abs/2107.03006v2>.
- Dhariwal, P. and Nichol, A. Diffusion models beat gans on image synthesis. *Advances in Neural Information Processing Systems*, 11:8780–8794, 5 2021. ISSN 10495258. doi: 10.48550/arxiv.2105.05233. URL <https://arxiv.org/abs/2105.05233v4>.
- Dockhorn, T., Vahdat, A., and Kreis, K. Score-based generative modeling with critically-damped langevin diffusion. 12 2021. doi: 10.48550/arxiv.2112.07068. URL <https://arxiv.org/abs/2112.07068v4>.
- Ho, J., Jain, A., and Abbeel, P. Denoising diffusion probabilistic models. *Advances in Neural Information Processing Systems*, 2020-December, 6 2020. ISSN 10495258. doi: 10.48550/arxiv.2006.11239. URL <https://arxiv.org/abs/2006.11239v2>.
- Ho, J., Research, G., and Salimans, T. Classifier-free diffusion guidance, 11 2021.
- Ho, J., Salimans, T., Gritsenko, A., Chan, W., Norouzi, M., and Fleet, D. J. Video diffusion models. 4 2022. doi: 10.48550/arxiv.2204.03458. URL <https://arxiv.org/abs/2204.03458v2>.
- Hoogeboom, E., Nielsen, D., Jaini, P., Forré, P., and Welling, M. Argmax flows and multinomial diffusion: Learning categorical distributions. *Advances in Neural Information Processing Systems*, 15:12454–12465, 2 2021. ISSN 10495258. doi: 10.48550/arxiv.2102.05379. URL <https://arxiv.org/abs/2102.05379v3>.
- Jo, J., Lee, S., and Hwang, S. J. Score-based generative modeling of graphs via the system of stochastic differential equations. 2 2022. doi: 10.48550/arxiv.2202.02514. URL <https://arxiv.org/abs/2202.02514v3>.
- Karras, T., Aittala, M., Aila, T., and Laine, S. Elucidating the design space of diffusion-based generative models. 6 2022. doi: 10.48550/arxiv.2206.00364. URL <https://arxiv.org/abs/2206.00364v1>.
- Kong, Z. and Ping, W. On fast sampling of diffusion probabilistic models. 5 2021. doi: 10.48550/arxiv.2106.00132. URL <https://arxiv.org/abs/2106.00132v1>.
- Kong, Z., Ping, W., Huang, J., Zhao, K., Research, B., and Catanzaro, B. Diffwave: A versatile diffusion model for audio synthesis. 9 2020. doi: 10.48550/arxiv.2009.09761. URL <https://arxiv.org/abs/2009.09761v3>.
- Kotelnikov, A., Baranchuk, D., Rubachev, I., and Babenko, A. Tabddpm: Modelling tabular data with diffusion models. 9 2022. doi: 10.48550/arxiv.2209.15421. URL <https://arxiv.org/abs/2209.15421v1>.
- Lee, S., Jo, J., Hwang, S. J., and Korea, S. Exploring chemical space with score-based out-of-distribution generation. 6 2022. doi: 10.48550/arxiv.2206.07632. URL <https://arxiv.org/abs/2206.07632v1>.
- Niu, C., Song, Y., Song, J., Zhao, S., Grover, A., and Ermon, S. Permutation invariant graph generation via score-based generative modeling. 3 2020. doi: 10.48550/arxiv.2003.00638. URL <https://arxiv.org/abs/2003.00638v1>.
- Patterson, D., Gonzalez, J., Le, Q., Liang, C., Munguia, L.-M., Rothchild, D., So, D., Texier, M., and Dean, J. Carbon emissions and large neural network training. 4 2021. doi: 10.48550/arxiv.2104.10350. URL <https://arxiv.org/abs/2104.10350v3>.
- Rombach, R., Blattmann, A., Lorenz, D., Esser, P., and Ommer, B. High-resolution image synthesis with latent diffusion models. 12 2021. doi: 10.48550/arxiv.2112.10752. URL <https://arxiv.org/abs/2112.10752v2>.
- Sohl-Dickstein, J., Weiss, E. A., Maheswaranathan, N., and Ganguli, S. Deep unsupervised learning using nonequilibrium thermodynamics. *32nd International Conference on Machine Learning, ICML 2015*, 3:2246–2255, 3 2015. doi: 10.48550/arxiv.1503.03585. URL <https://arxiv.org/abs/1503.03585v8>.
- Song, Y., Sohl-Dickstein, J., Brain, G., Kingma, D. P., Kumar, A., Ermon, S., and Poole, B. Score-based generative modeling through stochastic differential equations. 2021.
- Strubell, E., Ganesh, A., and McCallum, A. Energy and policy considerations for modern deep learning research. *Proceedings of the AAAI Conference on Artificial Intelligence*, 34:13693–13696, 4 2020. ISSN 2374-3468. doi: 10.1609/AAAI.V34I09.7123. URL <https://ojs.aaai.org/index.php/AAAI/article/view/7123>.
- Vahdat, A., Kreis, K., and Kautz, J. Score-based generative modeling in latent space. *Advances in Neural Information Processing Systems*, 14:11287–11302, 6 2021. ISSN 10495258. doi: 10.48550/arxiv.2106.05931. URL <https://arxiv.org/abs/2106.05931v3>.

van de Ven, G. M. and Tolias, A. S. Three scenarios for continual learning. 4 2019. doi: 10.48550/arxiv.1904.07734. URL <https://arxiv.org/abs/1904.07734v1>.

Watson, D., Ho, J., Norouzi, M., and Chan, W. Learning to efficiently sample from diffusion probabilistic models. 6 2021. doi: 10.48550/arxiv.2106.03802. URL <https://arxiv.org/abs/2106.03802v1>.

Xiao, Z., Kreis, K., and Vahdat, A. Tackling the generative learning trilemma with denoising diffusion gans. 12 2021. doi: 10.48550/arxiv.2112.07804. URL <https://arxiv.org/abs/2112.07804v2>.

## A. Supplementary Figures and Tables

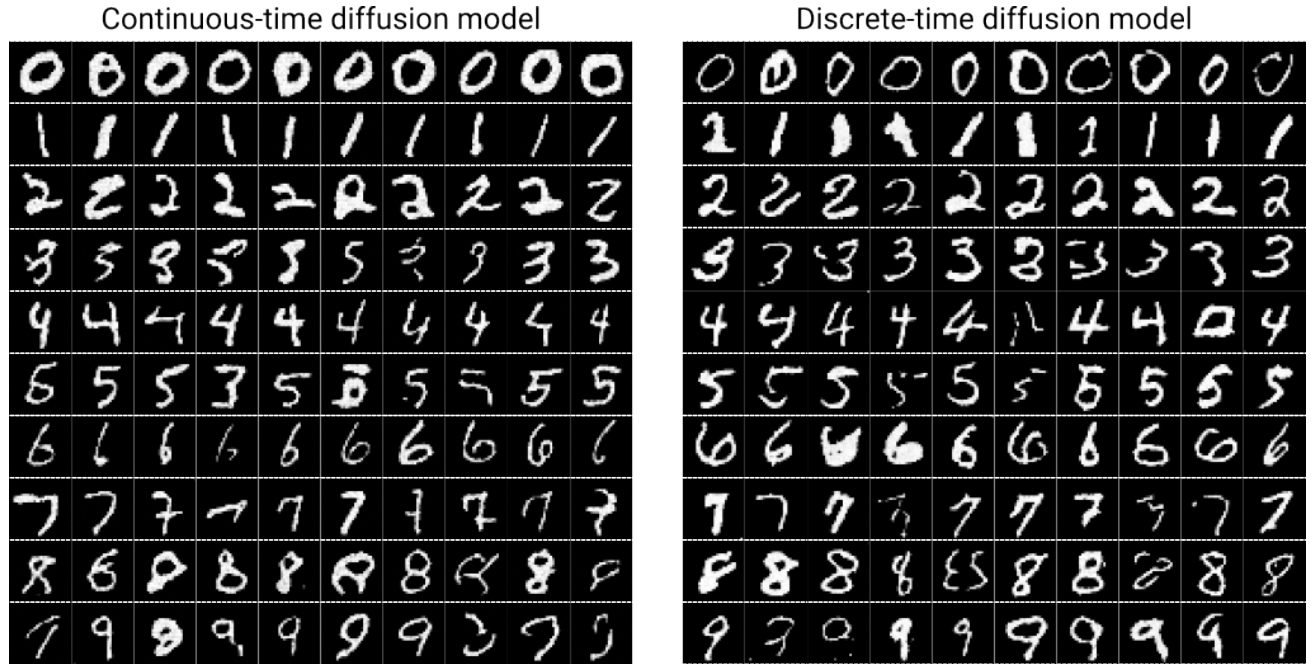
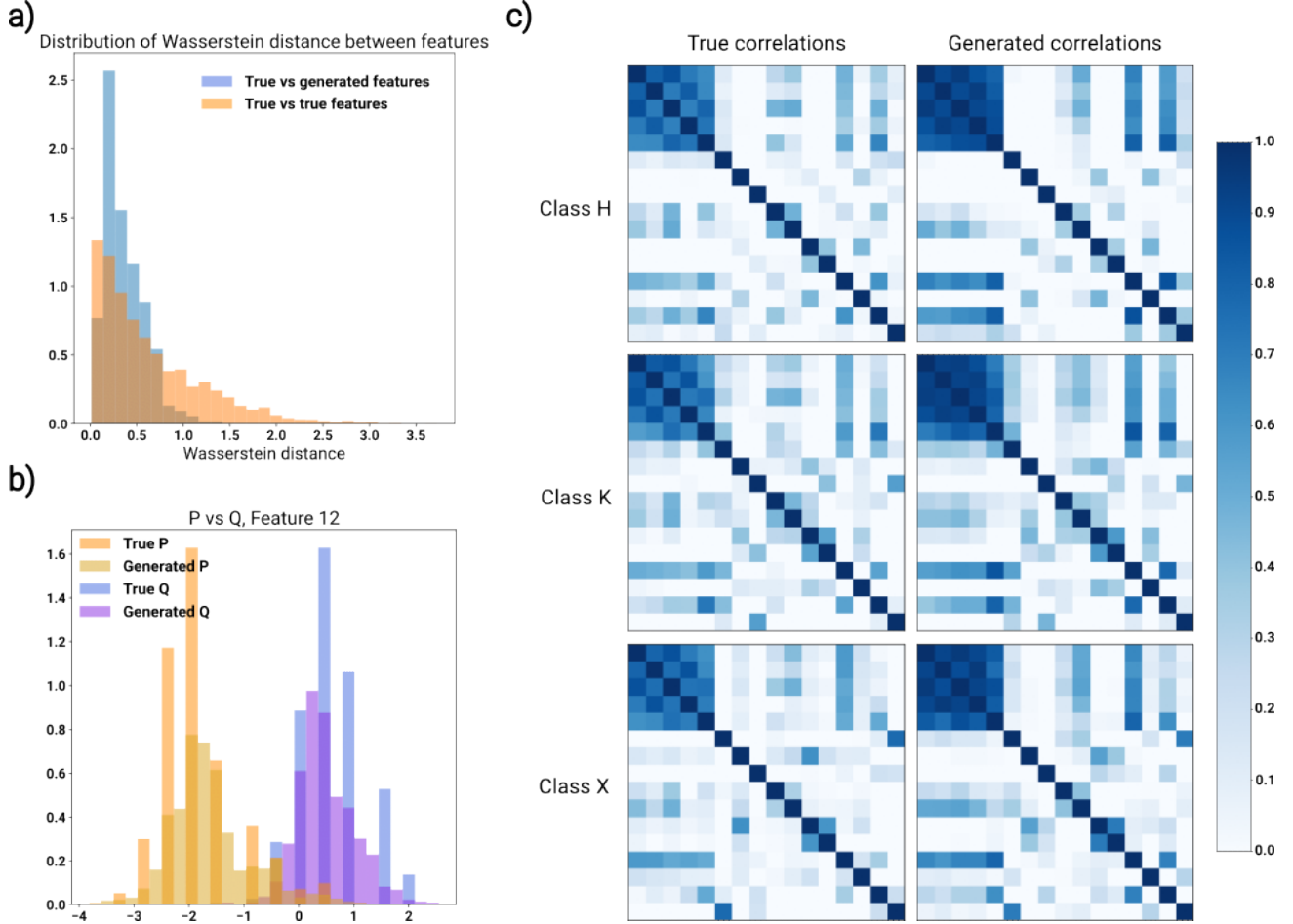


Figure S1. Examples of generated MNIST images. We show (uncurated) images of MNIST digits generated by branched diffusion models. Since branched diffusion models naturally output each class separately, generation of individual classes does not require supplying labels or pretrained classifiers. We show a sample of digits generated from a continuous-time (score-matching) diffusion model (Song et al., 2021), and a discrete-time diffusion model (denoising diffusion probabilistic model) (Ho et al., 2020). Branched diffusion models for multi-class generation fit neatly into practically any diffusion-model framework.



**Figure S2.** Examples of generated letters. We show some examples of distributions generated from a branched diffusion model trained on tabular data: English letters of various fonts, featurized by a hand-engineered set of 16 features. **a)** For each letter class and each of the 16 numerical features, we compute the Wasserstein distance (i.e. earthmover’s distance) between the true data distribution and the generated data distribution. We compare this distribution of Wasserstein distances to the distances between different true distributions of features as a baseline. On average, the branched diffusion model learns to generate features which are similar in distribution to the true data. **b)** We show an example of the true and generated feature distributions for a particular feature, comparing two letter classes: P and Q. Although the two classes show a very distinct distribution for this feature, the branched diffusion model captures this distinction well and correctly generates the feature distribution for each class. **c)** Over all 16 numerical features, we compute the Pearson correlation between the features, and compare the correlation heatmaps between the true data and the generated examples. In each of these three classes, the branched diffusion model has learned to capture not only the overarching correlational structure shared by all three classes, but also the subtle secondary correlations unique to each class.



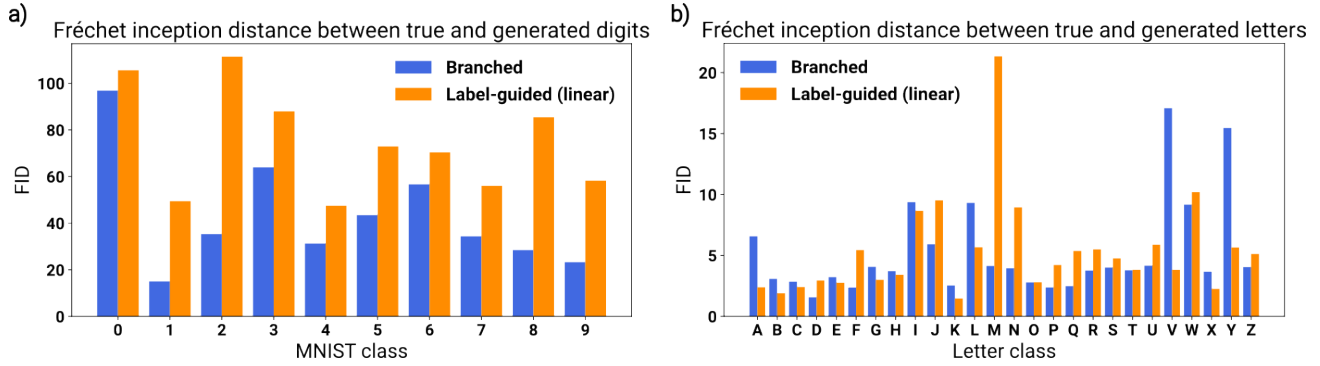


Figure S3. Sample quality of branched diffusion vs label-guided (linear) diffusion. We compare the quality of generated data from branched diffusion models to label-guided (linear) diffusion models of similar capacity and architecture. During training and sample generation, the label-guided diffusion model was trained with a class label as an auxiliary input at each stage of the reverse-diffusion process. For each class, we computed the Fréchet inception distance (FID) between the generated examples and a sample of the true data. A lower FID is better. We show the FID for generated **a)** MNIST digits and **b)** tabular letters. We find that our branched diffusion model achieves comparable sample quality compared to the current state-of-the-art method of label-guided diffusion. In some cases, the branched model may even generate consistently better examples.

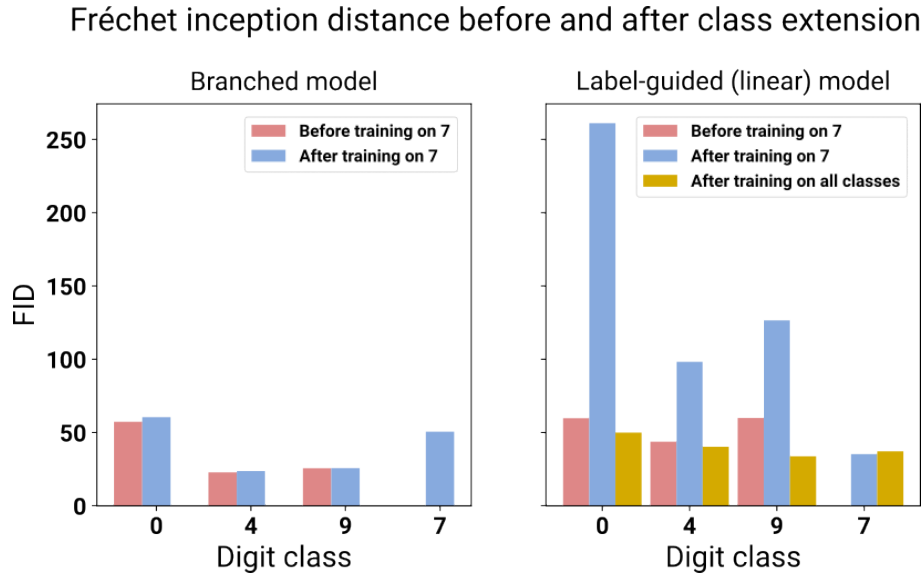


Figure S4. MNIST sample quality before and after class extension. Starting with diffusion models trained to generate 0s, 4s, and 9s, we extended the models to accommodate a new digit class: 7. We show the Fréchet inception distance (FID) between the generated examples and a sample of the true data. A lower FID is better. For the branched diffusion model (left), the FIDs of pre-existing classes are effectively unchanged before versus after training on 7s. For the label-guided (linear) model (right), the FIDs are significantly worse due to the model's catastrophic forgetting. In order to recover good-quality samples of all digit classes, the linear model needs to be further trained on the entire dataset.

Table S1. MNIST (continuous) branch definitions

BRANCH START ( $s_i$ )	BRANCH END ( $t_i$ )	BRANCH CLASSES ( $C_i$ )
0.4855	1	0,1,2,3,4,5,6,7,8,9
0.4474	0.4855	1,2,3,4,5,6,7,8,9
0.4334	0.4474	2,3,4,5,6,7,8,9
0.4164	0.4334	2,3,4,5,7,8,9
0.3744	0.4164	3,4,5,7,8,9
0.3684	0.3744	3,4,5,8,9
0.3524	0.3684	3,4,5,9
0.3483	0.3524	3,4,5
0.2713	0.3483	3,5
0	0.4855	0
0	0.4474	1
0	0.4334	6
0	0.4164	2
0	0.3744	7
0	0.3684	8
0	0.3524	9
0	0.3483	4
0	0.2713	5
0	0.2713	3

Branch definitions for continuous-time model on all MNIST digits.

Table S2. MNIST (discrete) branch definitions

BRANCH START ( $s_i$ )	BRANCH END ( $t_i$ )	BRANCH CLASSES ( $C_i$ )
761	1000	0,1,2,3,4,5,6,7,8,9
760	761	0,2,3,4,5,6,7,8,9
712	760	2,3,4,5,6,7,8,9
709	712	3,4,5,6,7,8,9
700	709	3,5,6,8
685	709	4,7,9
659	700	3,5,8
656	659	3,5
527	685	4,9
0	761	1
0	760	0
0	712	2
0	700	6
0	685	7
0	659	8
0	656	5
0	656	3
0	527	4
0	527	9

Branch definitions for discrete-time model on all MNIST digits.

Table S3. MNIST (continuous) branch definitions for 0, 4, and 9

BRANCH START ( $s_i$ )	BRANCH END ( $t_i$ )	BRANCH CLASSES ( $C_i$ )
0.5	1	0,4,9
0	0.5	0
0.35	0.5	4,9
0	0.35	4
0	0.35	9

Branch definitions for continuous-time model on MNIST digits 0, 4, and 9.

Table S4. MNIST (continuous) branch definitions for 0, 4, 7, and 9

BRANCH START ( $s_i$ )	BRANCH END ( $t_i$ )	BRANCH CLASSES ( $C_i$ )
0.5	1	0,4,7,9
0	0.5	0
0.38	0.5	4,7,9
0	0.38	7
0.35	0.38	4,9
0	0.35	4
0	0.35	9

Branch definitions for continuous-time model on MNIST digits 0, 4, 7, and 9.

Table S5. Letters (continuous) branch definitions

BRANCH START ( $s_i$ )	BRANCH END ( $t_i$ )	BRANCH CLASSES ( $C_i$ )
0.5235	1	A,B,C,D,E,F,G,H,I,J,K,L,M,N,O,P,Q,R,S,T,U,V,W,X,Y,Z
0.5165	0.5235	A,B,C,D,E,F,G,H,I,J,K,L,M,N,O,P,Q,R,S,T,U,V,X,Y,Z
0.5115	0.5165	B,C,D,E,F,G,H,I,J,K,L,M,N,O,P,Q,R,S,T,U,V,X,Y,Z
0.4945	0.5115	B,C,D,E,F,G,H,I,J,K,M,N,O,P,Q,R,S,T,U,V,X,Y,Z
0.4795	0.4945	I,J
0.4725	0.4945	B,C,D,E,F,G,H,K,M,N,O,P,Q,R,S,T,U,V,X,Y,Z
0.4565	0.4725	B,C,D,E,G,H,K,M,N,O,Q,R,S,U,X,Z
0.4364	0.4725	F,P,T,V,Y
0.4174	0.4565	B,C,D,E,G,H,K,N,O,Q,R,S,U,X,Z
0.4134	0.4174	B,C,D,E,G,H,K,N,O,Q,R,S,X,Z
0.4094	0.4134	B,D,G,H,K,N,O,Q,R,S,X,Z
0.4024	0.4364	F,T,V,Y
0.3864	0.4094	B,D,G,H,K,O,Q,R,S,X,Z
0.3814	0.3864	B,G,H,K,O,Q,R,S,X,Z
0.3734	0.3814	B,G,H,O,Q,R,S,X,Z
0.3604	0.4024	F,T,Y
0.3564	0.4134	C,E
0.3534	0.3604	T,Y
0.3514	0.3734	B,R,S,X,Z
0.3413	0.3734	G,H,O,Q
0.3223	0.3514	B,S,X,Z
0.2763	0.3223	B,S,X
0.2643	0.3413	G,H,O
0.2573	0.2643	G,O
0.1562	0.2763	S,X
0	0.5235	W
0	0.5165	A
0	0.5115	L
0	0.4795	J
0	0.4795	I
0	0.4565	M
0	0.4364	P
0	0.4174	U
0	0.4094	N
0	0.4024	V
0	0.3864	D
0	0.3814	K
0	0.3604	F
0	0.3564	E
0	0.3564	C
0	0.3534	Y
0	0.3534	T
0	0.3514	R
0	0.3413	Q
0	0.3223	Z
0	0.2763	B
0	0.2643	H
0	0.2573	G
0	0.2573	O
0	0.1562	S
0	0.1562	X

Branch definitions for continuous-time model on all letters.



Table S6. Relative size and capacity of branched models vs relative training time

BRANCHED DIFFUSION MODEL	TOTAL BRANCH LENGTH	APPROXIMATE MODEL CAPACITY	ACTUAL TRAINING TIME
MNIST (CONTINUOUS TIME)	11.49	11	3
MNIST (DISCRETE TIME)	19.51	11	2
LETTERS (CONTINUOUS TIME)	30.14	27	3

Because branched diffusion models separate the diffusion process into branches, they naturally often require more epochs to train than their linear counterparts. We found, however, that the time taken to train these models was still far less than what would be expected if the training time were an additive function of total branch length or model capacity. Here, we show (for each of our main branched models) the total branch length (i.e. sum of all branch diffusion times), the approximate model capacity, and the actual training time in epochs. All values in the table above are *relative* (i.e. divided by) the branched model’s linear counterpart. Although training time for branched models was already far less than what is expected based on branch length or model capacity, we also suggest that training with larger batch sizes or accumulating gradient updates between batches (particularly for shorter branches) may also allow for these models to be trained even faster. We leave exploration of this for future work.

## B. Supplementary Methods

The code to generate the results and figures in this work is available at <https://github.com/Genentech/Branched-Diffusion>.

We trained all of our models and performed all analyses on a single Nvidia Quadro P6000.

### B.1. Training data

We downloaded the MNIST dataset and used all digits from <http://yann.lecun.com/exdb/mnist/>. We rescaled and recentered the values from  $[0, 255]$  to  $[-1, 1]$ . This rescaling and symmetrization about 0 was to assist in the forward-diffusion process, which adds noise until the distribution approaches a standard (0-mean, identity-covariance) Gaussian.

We downloaded the tabular letter-recognition dataset from the UCI repository: <https://archive.ics.uci.edu/ml/datasets/Letter+Recognition>. We centered and scaled each of the 16 tabular features to 0 mean and unit variance (pooled over the entire dataset, not for each individual letter class).

### B.2. Diffusion processes

For all of our continuous-time diffusion models, we employed the “variance-preserving stochastic differential equation” (VP-SDE) (Song et al., 2021). We used a variance schedule of  $\beta(t) = 0.9t + 0.1$ . We set our time horizon  $T = 1$  (i.e.  $t \in [0, 1]$ ). This amounts to adding Gaussian noise over continuous time.

For our discrete-time diffusion model, we defined a discrete-time Gaussian noising process, following Ho et al. (2020). We defined  $\beta_t = (1 \times 10^{-4}) + (1 \times 10^{-5})t$ . We set our time horizon  $T = 1000$  (i.e.  $t = [0, 1000]$ ).

### B.3. Defining branches

In a branched diffusion model, each branch  $b_i = (s_i, t_i, C_i)$  learns to reverse diffuse between times  $[s_i, t_i]$  for classes in  $C_i$ . The branches form a tree structure (i.e. hierarchy) with the root at time  $T$  and a branch for each individual class at time 0. These branch definitions may come from prior domain knowledge, or they can be computed from the training data alone. For our models, we computed the branch definitions using the following algorithm:

1. Start with a dataset of objects to generate, consisting of classes  $C$ .
2. For each class, sample  $n$  objects randomly and without replacement.
3. Forward diffuse each object over every time point in the forward-diffusion process (e.g. in our models, we had 1000 forward-diffusion steps). The branched diffusion model which will be trained using these branch definitions employs an identical forward-diffusion process.
4. At each time point  $t$ , compute the average similarity of each pair of classes, resulting in a  $|C| \times |C|$  similarity matrix at each of the 1000 time points. For distinct classes  $c_i, c_j$  ( $i \neq j$ ), the similarity  $s(t, c_i, c_j)$  is computed over the average of  $n$  pairs, where the pairs are randomly assigned between the two classes; for self-similarity of class  $c_i$ , the similarity  $s(t, c_i, c_i)$  is computed over the average of  $n$  pairs within the class, randomly assigned such that the same object is not compared with itself. For simplicity, the similarity metric we used was Euclidean distance over the flattened vectors, but other metrics may be used which better match the domain.
5. For each pair of classes  $c_i, c_j$  ( $i$  may be equal to  $j$ ), smooth the trajectory of  $s(t, c_i, c_j)$  over time by applying a Gaussian smoothing kernel of standard deviation equal to 3 and truncated to 4 standard deviations on each side.
6. For each pair of *distinct* classes  $c_i, c_j$  ( $i \neq j$ ), compute the *earliest* time in the forward-diffusion process such that the average similarity between  $c_i$  and  $c_j$  is at least the self-similarity of  $c_i$  and  $c_j$  (averaged between the two). A tolerance of  $\epsilon$  is allowed. That is, for each pair of distinct classes  $c_i, c_j$  ( $i \neq j$ ), compute the *minimum*  $t$  such that  $s(t, c_i, c_j) \geq \frac{1}{2}(s(t, c_i, c_i) + s(t, c_j, c_j)) - \epsilon$ . This gives each pair of distinct classes a “minimal time of indistinguishability”,  $\tau_{c_i, c_j}$ .
7. Order the  $\binom{|C|}{2}$  minimal times of indistinguishability  $\tau$  by ascending order, and greedily build a hierarchical tree by merging classes together if they have not already been merged. This can be implemented by a set of  $|C|$  disjoint sets,

where each set contains one class; iterating through the times  $\tau$  in order, two branches merge into a new branch by merging together the sets containing the two classes, unless they are already in the same set.

For our continuous-time branched model on MNIST, we used  $\epsilon = 0.005$ . For our discrete-time branched model on MNIST, we used  $\epsilon = 0.001$ . For our continuous-time branched model on tabular letters, we used  $\epsilon = 0.01$ . These values were selected such that the branch points were not all too close to 0 or  $T$ .

The final branch definitions can be found in the Supplementary Figures and Tables.

#### B.4. Model architectures

Our model architectures are designed after the architectures presented in [Song et al. \(2021\)](#) and [Kotelnikov et al. \(2022\)](#).

Our MNIST models were trained on a UNet architecture consisting of 4 downsampling and 4 upsampling layers. In our branched models, the upsampling layers were shared between output tasks. We performed group normalization after every layer. The time embedding was computed as  $[\sin(2\pi \frac{t}{T}), \cos(2\pi \frac{t}{T})]$ . For each layer in the UNet, the time embedding was passed through a separate dense layer (unique for every UNet layer) and concatenated on the input to the UNet layer. For a label-guided model, we learned an embedding for each discrete label. As with the time embedding, the label embedding was passed through a separate dense layer (unique for every UNet layer) and concatenated on the input to each UNet layer.

Our letter models were trained on a dense architecture consisting of 5 dense layers. In our branched models, the first two layers were shared between output tasks. The time embedding was computed as  $[\sin(2\pi \frac{t}{T} z), \cos(2\pi \frac{t}{T} z)]$ , where  $z$  is a set of Gaussian parameters that are not trainable. The time embeddings were passed through a dense layer, and the output was added onto the input after the first dense layer. For a label-guided model, we again learned an embedding for each discrete label. The label embedding was passed through a dense layer, and the result was concatenated onto the summation of the time embedding and the input after the first layer, before being passed to the remaining 4 layers.

#### B.5. Training schedules

For all of our models, we trained with a batch size of 128 examples, drawing uniformly from the entire dataset. This naturally ensures that branches which are longer (i.e. take up more diffusion time) or are responsible for more classes are upweighted appropriately.

For all of our models, we used a learning rate of 0.001.

For our label-guided MNIST model, we trained for 30 epochs, and we noted that the loss had converged at that point. For our label-guided letters models, we trained for 100 epochs, again noting that the loss had converged at that point.

For our branched continuous-time MNIST model, we trained for 90 epochs. For our branched discrete-time MNIST model, we trained for 200 epochs. For our branched letter model (continuous-time), we trained for 300 epochs.

For our analysis on extending branched models and label-guided (linear) models to new classes, we also trained MNIST models on a subset of the dataset (i.e. only 0/4/9 or only 0/4/7/9). In these cases, we followed the same training parameters as above, except we trained for fewer epochs. In the class-extension analyses, we started with branched or label-guided models trained on 0s, 4s, and 9s. These models we trained for 30 epochs each. We then fine-tuned these models by training only a single branch of the branched model or the entire linear model, on only 7s or on all four digits. When fine-tuning, we also used the same training details as above, but we only trained for 10 epochs.

#### B.6. Sampling procedure

When generating samples from a continuous-time diffusion model, we used the predictor-corrector algorithm defined in [Song et al. \(2021\)](#), using 1000 time steps from  $T$  to 0. For our discrete-time diffusion model, we used the sampling algorithm defined in [Ho et al. \(2020\)](#). Note that we employed Algorithm 2 for branched models.

#### B.7. Analyses

##### *Sample quality*

We compared the quality of samples generated from our branched diffusion models to those generated by our label-guided

(linear) diffusion models using Fréchet Inception Distance (FID). For each class, we generated 1000 samples of each class from the branched model, 1000 samples of each class from the linear model, and 1000 samples of each class from the true dataset. We computed FID over these samples, comparing each set of generated classes against the true samples. For the tabular letters dataset, there were not enough letters in the dataset to draw 1000 true samples of each letter, so we drew 700 of each letter from the true dataset.

#### *Sampling efficiency*

We computed the amount of time taken to generate 64 of each class from our branched diffusion models, with and without taking advantage of the branch points. We took the average time taken over 10 trials each.

When leveraging the branching structure to generate samples, we ordered the branches by start time  $s_i$  in *descending* order. For each branch  $b_i$  in order, we reverse diffused down the branch, starting with a cached intermediate at  $t_i$  for the branch that ended at  $t_i$ . For the very first branch (the root), we started reverse diffusion by sampling  $\pi(x)$ . This guarantees that we will have a cached batch of samples at every branch point before we encounter a branch that starts at that branch point. Eventually, this algorithm generates a batch of samples for each class. For each branch, we performed reverse diffusion such that the total number of steps for any one class from  $t = T$  to  $t = 0$  was 1000.

To generate samples without leveraging the branching structure, we simply generated each class separately from the branched model, without caching any intermediates. Note that this takes the same amount of time as a purely linear model (of identical capacity and architecture) without any branching structure.

#### *Class extension*

To extend a new branch to reverse diffuse 7s on our branched diffusion model on 0s, 4s, and 9s, we simply created a new model with one extra output task and copied over the corresponding weights. For the new branch, we initialized the weights to the same as those on the corresponding 9 branch (with  $s_i = 0$ ). We trained this new branch for 10 epochs on only 7s, only for the time interval of that new branch.

On the corresponding label-guided (linear) model, we fine-tuned on only 7s or on 0s, 4s, 7s, and 9s. In each experiment, we started with the linear model trained on 0s, 4s, and 9s, and trained for 10 epochs. Note that training on all four digits had many more batches for each epoch due to the larger dataset size.

#### *Hybrid intermediates and transmutation*

For certain pairs of MNIST digits or letters, we found the earliest branch point for which they belong to the same branch, and generated hybrids by reverse-diffusing to that branch point. Transmuted objects were computed by forward diffusing from one class to this branch point, and then reverse diffusing down the path to the other class from that intermediate.